

Spin density functional study of magnetism in potassium-loaded zeolite A

Yoshiro Nohara,¹ Kazuma Nakamura,² and Ryotaro Arita²

¹*Department of Physics, University of Tokyo, Tokyo 113-0022, Japan*

²*Department of Applied Physics, University of Tokyo, Tokyo 113-0033, Japan*

(Received 2 October 2009; published 28 December 2009)

In order to clarify the mechanism of spin polarization in potassium-loaded zeolite A, we perform *ab initio* density functional calculations. We find that (i) the system comprising only nonmagnetic elements (Al, Si, O, and K) can indeed exhibit ferromagnetism, (ii) the host cage makes a confining quantum-well potential in which superatom *s*- and *p*-like states are formed, the latter *p* states are responsible for the spin polarization, and (iii) the size of the magnetic moment depends sensitively on atomic positions of potassium clusters. We show that the spin polarization can be described systematically in terms of the confining potential and the crystal-field splitting in the superatom *p* states.

DOI: [10.1103/PhysRevB.80.220410](https://doi.org/10.1103/PhysRevB.80.220410)

PACS number(s): 75.75.+a, 73.22.-f, 82.75.Vx

Searching for ferromagnets comprising only nonmagnetic elements has been a fascinating challenge in condensed-matter physics. Motivated by fundamental interests or potential technological importance, various ferromagnets with nonmagnetic elements have been synthesized.^{1,2} Among them, alkali-metal-loaded zeolites are certainly unique ferromagnets. Depending on the crystal structure of the host cage and the number or species of the guest-cluster atoms, they exhibit not only ferromagnetism but also a rich variety of magnetic properties.^{3,4} In fact, one can envisage to design and control the magnetic properties of this system by choosing appropriate combinations of the guests and hosts.⁵

The first step we should take is to understand the mechanism of the spin polarization in this system. Indeed, it is of great interest to consider why clusters of alkali atoms confined in zeolite cages can be magnetic even though the bulk alkali metals are nonmagnetic. However, while almost 20 years have passed since the seminal discovery of the spin-polarized ground state in zeolite A,³ *ab initio* studies on magnetism in zeolitic materials have been quite limited so far except for sodalites having the smallest unit cell.⁶ This is mainly because (i) the electronic structure is expected to be very complicated since the unit cell of the system is huge [typically it has $O(100)$ atoms and the lattice constant is ~ 30 Å] and (ii) the atomic positions has not been determined accurately in experiments due to the extreme complexity in the structure of the system.

However, fortunately, the situation of potassium-loaded zeolite A ($K_{12+n}Si_{12}Al_{12}O_{48}$, hereafter we call it as K-LTA) is different; a detailed neutron powder-diffraction study has been performed,⁷ and thus we exceptionally have a reliable reference for *ab initio* calculations. On top of that, recent density functional calculations based on local-density approximation (LDA) have clarified that the low-energy electronic structure of this compound is quite simple.⁵ Namely, the system is regarded as a *supercrystal*, where guest-potassium clusters act as a *superatom* with well-defined *s*- and *p*-like orbitals.⁸ Thus, the low-energy physics is expected to be described systematically in terms of the superatom picture.

Experimentally, the spin polarization in K-LTA is observed when we introduce more than two potassium atoms (i.e., $n > 2$) and the Curie and Weiss temperature take their

maximum at $n \sim 4$. If we follow the picture mentioned above, the superatom *s* state is fully occupied and three *p* states are partially filled for $n \sim 4$. While several scenarios for the spin states in K-LTA, considering the orbital degeneracy of the *p* states, have been proposed,⁹⁻¹¹ *ab initio* calculations based on spin density functional theory have yet to be done.

The purpose of this Rapid Communication is thus to clarify the mechanism of spin polarization in K-LTA from first principles. We examine in detail (i) whether a ferromagnetic ground state is in fact realized just from Si, Al, O, and K and (ii) if it does, for which condition the system has spin polarization. Hereafter, we focus on the case of $n=4$, where the energy scale of magnetism is expected to be largest.

Let us consider a detail of the atomic positions in this Rapid Communication. Figure 1 shows the atomic geometry determined by the neutron measurement with an assumption that the system has the symmetry of space group $F23$.⁷ Due to the Lowenstein rule (Si and Al should be arranged alternately), the unit cell contains two large (small) aluminosilicate cages which we call α (β) cages (upper left panel). While the previous LDA calculation employed a simplified unit cell having only one α and β cage (which violates the Lowenstein rule),⁵ here we adopt the original unit cell having 176 atoms. Hereafter, we label the two α cages as α_1 and α_2 (upper right panel). While the positions of Al, Si, and O were uniquely determined by the measurement, the experiment found several possible positions for potassium atoms in the α cages (bottom panel). Following this observation, we denote the center of six-, four-, and eight-membered rings in the α cage as site I,¹² II, and III, respectively. The site IV is the center of the α cage. In order to indicate which α cage the site I, III, and IV belong to, we label them with subscript such as site I_{α_1} or I_{α_2} . Notice that the site II is on the border of two α cages.

The experimental occupation numbers of site I_{α_1} , I_{α_2} , II, III_{α_1} , III_{α_2} , IV_{α_1} , and IV_{α_2} are 8.0, 8.0, 6.4, 5.9, 3.5, 0.0, and 0.5, respectively. In the present calculation, for simplicity, we assume the occupation numbers as 8, 8, 6, 6, 3, 0, and 1. Thus, the sites I, II, and IV_{α_2} are fully occupied and the site IV_{α_1} is completely vacant. Note that the total number of the potassium atoms in the unit cell is 32 in which the number of

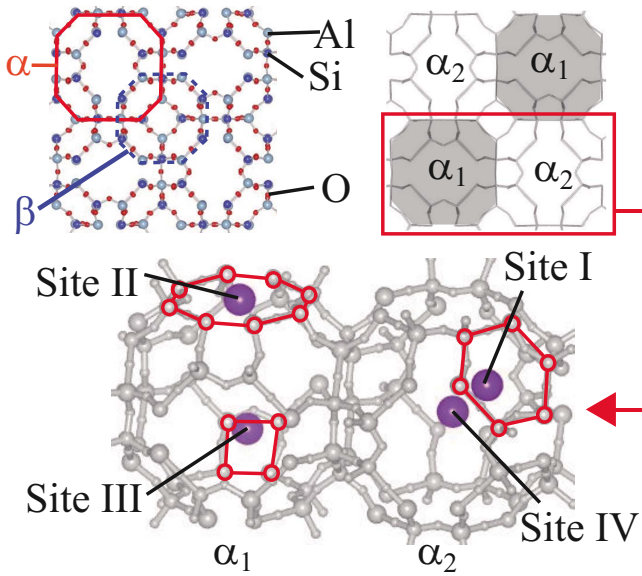


FIG. 1. (Color online) Upper left: overall profile of zeolite LTA, where O, Al, and Si atoms are denoted by small red, light blue, and dark blue spheres, respectively. α and β cages are marked by (red) solid and (blue) dashed lines, respectively. Upper right: two kinds of α cages (α_1 and α_2). Lower panel: four kinds of sites occupied by potassium [(purple) large spheres]. For the definition of the sites I-IV, see the text.

sites I, II, and III is 16, 6, and 24, respectively. While the atomic positions of the sites I, II and IV are uniquely determined, there are huge possibilities for the configuration of the site III; since there are 24 possible positions and we have nine potassium atoms in the site III (six for the α_1 cage and three for the α_2 cage), we have ${}_{12}C_6 \times {}_{12}C_3 = 203\,280$ possibilities. In this Rapid Communication, we focus on the following four geometries I-IV with trigonal symmetry shown in Fig. 2. Notice that this symmetry would be favored, due to the same symmetry of the confining aluminosilicate cage. We also note that the listed geometries I-IV cover all possible geometries with the trigonal symmetry. In those geometries, we have two triangles and a hexagon in the α_1 cage and a small triangle and a large triangle in the α_2 cage. Notice that, for the geometries I and III, the site-III and site-IV potassium in the α_2 cage form a tetrahedron.

Ab initio calculations based on generalized gradient approximation (GGA) (Ref. 13) were performed with *Tokyo Ab initio Program Package*.¹⁴ We used GGA exchange-correlation functional, plane-wave basis set and the ultrasoft pseudopotentials¹⁵ in the Kleinman-Bylander representation.¹⁶ The pseudopotential of potassium was supplemented by the partial core correction.¹⁷ The energy cutoff of plane waves representing wave functions is 36 Ry and a $4 \times 4 \times 4$ k -point sampling is employed. We adopted the atomic positions of experimental geometry without the structure optimization.

We show in Table I the total energies calculated for the geometries I-IV, together with local magnetic moments in each α cage.¹⁸ We see that the site-III configuration affects significantly the energetics and the value of the magnetic moment. Interestingly, for all the geometries, the moment

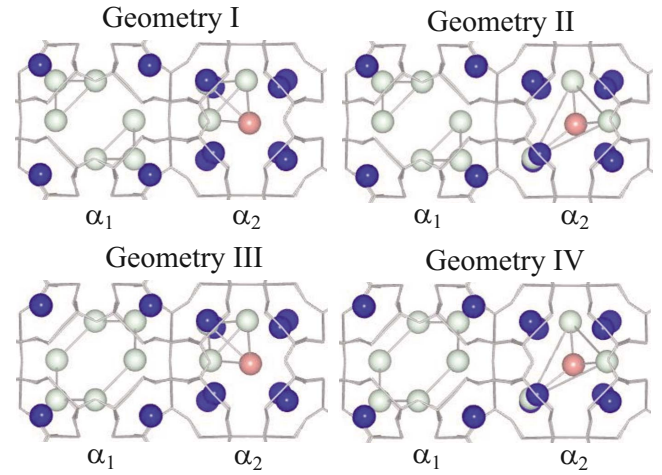


FIG. 2. (Color online) Four geometries considered in this Rapid Communication, where dark (blue), light (green), and medium (red) spheres stand for the potassiums occupying the site I, III, and IV, respectively. The difference in each geometry comes from the difference in the configuration of site-III potassiums; “two triangles” and “small triangle” (geometry I), “two triangles” and “large triangle” (geometry II), “hexagon” and “small triangle” (geometry III), and “hexagon” and “large triangle” (geometry IV) are accommodated in the α_1 and α_2 cages. We note that four site-I potassium in the α_1 cage are overlapped with the remaining four site-I potassium in this view.

develops in the α_2 cage, which suggests that the valence electrons responsible for the magnetism reside mainly in the α_2 cage. This is because the confining potential of the α_2 cage is deeper than that of the α_1 cage; as seen from Fig. 2, the site-I potassium in the α_2 cage is more centered than those in the α_1 cage, which makes the electrostatic potential in the α_2 cage deeper.

Another important point in Table I is that the size of the magnetic moment depends on the atomic positions of the potassium cluster. In order to clarify its origin, we calculated the low-energy bands and their wave functions. In the upper left (right) panel in Fig. 3, we show the low-energy band structures near the Fermi level for the geometries I (II) having largest (smallest) magnetic moment, corresponding to the first (second) column in Table I. While the band structure is quite different for these two geometries, the Bloch wave functions at the Γ point ($\Psi_A - \Psi_D$) have common features; (i) they have large amplitudes in the α_2 cage due to the deeper cage potential in α_2 mentioned above and (ii) they widely spread in the α cage without localizing on any specific atoms

TABLE I. Total energy per unit cell of each geometry ΔE_{tot} with reference to that of the geometry I and the local magnetic moments M_i in the α_i cage ($i=1$ or 2) (Ref. 18). For the definition for the geometries I-IV, see Fig. 2.

	Geom I	Geom II	Geom III	Geom IV
ΔE_{tot} (eV)	0	1.02	1.49	0.12
M_1 (μ_B)	-0.02	-0.20	0.06	-0.16
M_2 (μ_B)	1.92	0.33	1.36	1.00

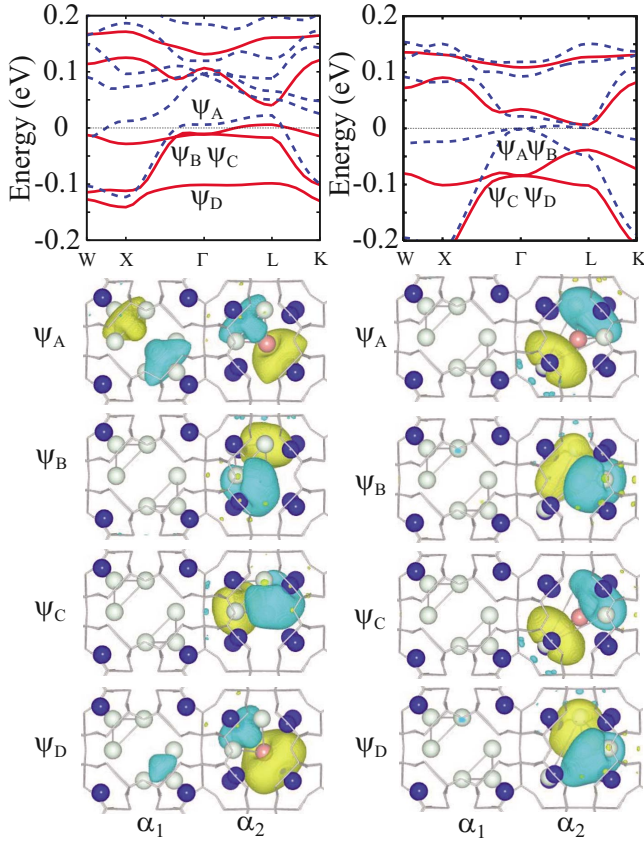


FIG. 3. (Color online) Calculated GGA band dispersions along symmetry lines [$W = \frac{2\pi}{a}(1, 0, \frac{1}{2})$, $X = \frac{2\pi}{a}(1, 0, 0)$, $\Gamma = \frac{2\pi}{a}(0, 0, 0)$, $L = \frac{2\pi}{a}(\frac{1}{2}, \frac{1}{2}, \frac{1}{2})$, and $K = \frac{2\pi}{a}(0, \frac{3}{4}, \frac{3}{4})$] (upper) and Bloch wave functions, $\Psi_A - \Psi_D$, at the Γ point (lower) for the geometries I (left) and II (right). In the band dispersion, (red) solid and (blue) dashed lines stand for majority and minority spin states, respectively. The energy zero is set to the Fermi level. In the wave functions, isosurfaces are drawn by the values of ± 0.015 (a.u.). Potassiums occupying the site I, III, and IV are displayed by spheres of the same colors with Fig. 2.

and are thus regarded as *superatom* p -type wave functions.⁵

To make the situation clearer, in Fig. 4, we draw level diagrams of the low-energy states, where the cage potentials, superatom p levels, and spin configurations are depicted schematically. Here, the p states are represented in the local coordinates, where the z axis is taken to be perpendicular to the triangles in α cages (see Fig. 2). In the geometry I (upper left in Fig. 4), for both the α cages, the superatom p_x and p_y levels are degenerated and higher than the p_z level; in the α_1 cage, the superatom p_z lobe extends in the direction of the center of the triangle and feels a positive crystal field, lowering the level of p_z . The same mechanism works in the α_2 cage, and thus the low-lying p_z states in α_1 and α_2 cages form a σ bonding orbital. On the other hand, the p_x and p_y states in the α_2 cage, with a nonbonding character, reside near the Fermi level. In the present case of $n=4$, there are four superatom p electrons. Two electrons accommodated in the σ bonding orbital and the remaining two electrons occupy the degenerated p_x and p_y orbitals. According to the Hund's rule, electron spins in the degenerated orbitals align

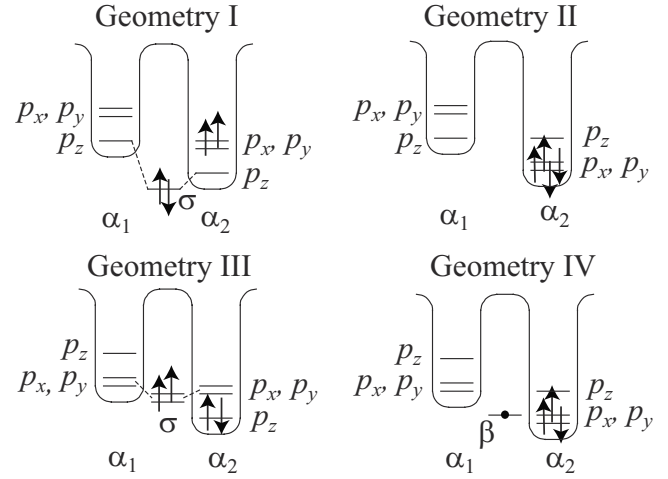


FIG. 4. Level diagrams for electronic structures of the four geometries displayed in Fig. 2, where superatom p levels in the α_1 - and α_2 -cage potentials and the resulting spin configurations are drawn schematically. The p states are represented in the local coordinates (for the definition, see the text). The difference between the cage potentials of α_1 and α_2 comes from the difference in the configuration of the site-I potassiums (see Fig. 2) and the p -level splitting is due to the site-III-potassium configurations.

to be parallel, thus generating the magnetic moment of $\sim 2 \mu_B$.

For the geometry II (upper right panel in Fig. 4), in the α_2 cage, the level of p_z is higher than p_x and p_y ; in this geometry, the p_x and p_y orbitals lie in the “large”-triangle plane and thus these states are stabilized electrostatically compared to the p_z state. Consequently, in the geometry II, the four electrons fully occupy the p_x and p_y states so that the system has hardly magnetic moments ($\sim 0 \mu_B$).

A similar argument can also hold in the cases of the geometries III and IV. In these geometries, the α_1 cage contains a hexagon instead of two triangles. The crystal field in the α_1 cage stabilizes the p_x and p_y states in the hexagon plane. In the geometry III (lower left panel in Fig. 4), the two electrons occupy the low-lying p_z orbital in the α_2 cage and the degenerated σ orbitals made from the p_x and p_y states in the α_1 and α_2 cages accommodate the remaining two electrons. Because the σ orbital is less localized, the value of the moment is somewhat reduced ($\sim 1.5 \mu_B$), compared to that of the geometry I. In the geometry IV (lower right panel), an extra state in the β cage appears near the Fermi level. This state was found to have a large dispersion and small spin polarization. The net moment is generated from the three electrons occupying the degenerated p_x and p_y orbitals, with the value of the moment $\sim \mu_B$. Here, we note that, for the geometry IV, not only the site I but also the site-IV potassium contributes to the formation of the moment; the presence of the site-IV atom leads to more localized p orbitals, thus making the moment size larger due to the large exchange splitting of the p orbital.

Thus, in this Rapid Communication, we found that K-LTA can be ferromagnetic in GGA and the mechanism of the spin polarization is consistently explained in view of the superatom picture; if the p levels formed by the superatom wave functions are degenerated and partially occupied, the system

becomes magnetic, due to the Hund's rule coupling in these states. This condition and the size of the moment are determined by the atomic positions of the guest potassium clusters, responsible for the cage-potential depth, and the crystal field inducing the p -level shift and split, respectively.

Experimentally, two kinds of possible scenarios for magnetic structures have been proposed for K-LTA. One is the ferrimagnetic model,¹¹ and the other is the spin-canted antiferromagnetic model.¹⁰ In the former, the system consists of two sublattices with large ($\sim 2.8\mu_B$) and small (almost $0.0\mu_B$) magnetic moment, while, in the latter, every α cage has a moment of μ_B . These magnetic structures look like the results for the geometries I and IV although the size of the moments is relatively smaller than the experimental values. It is interesting to note that the geometries I and IV have comparable energies (see Table I).

In reality, the site III is randomly occupied.⁷ It is definitely formidable to take into account the randomness of the site III explicitly in the first-principles calculations. On the other hand, our presented *ab initio* calculations have shown that the superatom picture works well in describing the low-energy physics of K-LTA. Thus, with this picture, a multi-orbital Hubbard-type model in the superatom p states with random potentials would be served as a realistic low-energy

model describing magnetism of the system. Since all the parameters characterizing the Hubbard model can be derived from first principles as was recently done in Ref. 19, we can discuss the magnetism in more realistic situations by solving this effective model. It will be an important future study.

To summarize, we found, by means of *ab initio* spin density functional calculations, that (i) K-LTA comprising only Al, Si, O, and K can be ferromagnetic, (ii) the superatom p states are responsible for the magnetism and (iii) the magnetic property of K-LTA depends sensitively on the atomic positions of the guest-potassium cluster. The condition for the spin polarization was presented and understood systematically in terms of the superatom picture. Our findings provide a firm basis and will be the first step for clarifying the low-energy physics in zeolitic materials.

We thank Yasuo Nozue, Takehito Nakano, and Mutsuo Igarashi for fruitful discussions. This work was supported by Scientific Research on Priority Areas of New Materials Science Using Regulated Nano Spaces (Grant No. 19051016) MEXT, Japan. All the computations have been performed on Hitachi SR11000 system at the Supercomputing Division, Information Technology Center, the University of Tokyo.

-
- ¹P.-M. Allemand, K. C. Khemani, A. Koch, F. Wudl, K. Holczer, S. Donovan, G. Grüner, and J. D. Thompson, *Science* **253**, 301 (1991).
- ²M. Takahashi, P. Turek, Y. Nakazawa, M. Tamura, K. Nozawa, D. Shiomi, M. Ishikawa, and M. Kinoshita, *Phys. Rev. Lett.* **67**, 746 (1991).
- ³Y. Nozue, T. Kodaira, and T. Goto, *Phys. Rev. Lett.* **68**, 3789 (1992); Y. Nozue, T. Kodaira, S. Ohwashi, T. Goto, and O. Terasaki, *Phys. Rev. B* **48**, 12253 (1993).
- ⁴V. I. Srdanov, G. D. Stucky, E. Lippmaa, and G. Engelhardt, *Phys. Rev. Lett.* **80**, 2449 (1998); T. Nakano, K. Goto, I. Watanabe, F. L. Pratt, Y. Ikemoto, and Y. Nozue, *Physica B* **374-375**, 21 (2006).
- ⁵R. Arita, T. Miyake, T. Kotani, M. van Schilfgaarde, T. Oka, K. Kuroki, Y. Nozue, and H. Aoki, *Phys. Rev. B* **69**, 195106 (2004).
- ⁶A. Monnier, V. Srdanov, G. Stucky, and H. Metiu, *J. Chem. Phys.* **100**, 6944 (1994); O. F. Sankey, A. A. Demkov, and T. Lenosky, *Phys. Rev. B* **57**, 15129 (1998); G. K. H. Madsen, B. B. Iversen, P. Blaha, and K. Schwarz, *ibid.* **64**, 195102 (2001); G. K. H. Madsen and P. Blaha, *ibid.* **67**, 085107 (2003).
- ⁷T. Ikeda, T. Kodaira, F. Izumi, T. Kamiyama, and K. Ohshima, *Chem. Phys. Lett.* **318**, 93 (2000).
- ⁸W. D. Knight, K. Clemenger, W. A. de Heer, W. A. Saunders, M. Y. Chou, and M. L. Cohen, *Phys. Rev. Lett.* **52**, 2141 (1984); W. Ekardt, *Phys. Rev. B* **29**, 1558 (1984).
- ⁹T. Nakano and Y. Nozue, *J. Comput. Methods Sci. Eng.* **7**, 443 (2007); T. Nakano, Doctoral thesis, Tohoku University, 2000.
- ¹⁰T. Nakano, D. Kiniwa, Y. Ikemoto, and Y. Nozue, *J. Magn. Magn. Mater.* **272-276**, 114 (2004).
- ¹¹H. Kira, H. Tou, Y. Maniwa, and Y. Murakami, *Physica B* **312-313**, 789 (2002).
- ¹²In the experiment, the exact position of a half of the site-I potassium is slightly different from the center of the six-membered ring and two positions for the site I have been observed. The occupancies are different (57% and 43%). In this Rapid Communication, we employ the high-probability position for all the site-I potassiums.
- ¹³J. P. Perdew, K. Burke, and M. Ernzerhof, *Phys. Rev. Lett.* **77**, 3865 (1996).
- ¹⁴J. Yamauchi, M. Tsukada, S. Watanabe, and O. Sugino, *Phys. Rev. B* **54**, 5586 (1996).
- ¹⁵D. Vanderbilt, *Phys. Rev. B* **41**, 7892 (1990).
- ¹⁶L. Kleinman and D. M. Bylander, *Phys. Rev. Lett.* **48**, 1425 (1982).
- ¹⁷S. G. Louie, S. Froyen, and M. L. Cohen, *Phys. Rev. B* **26**, 1738 (1982).
- ¹⁸The local magnetic moment of α cages was calculated for the Voronoi polyhedron having the same volume as that of the sphere of the radius of 7.64 Å.
- ¹⁹K. Nakamura, T. Koretsune, and R. Arita, *Phys. Rev. B* **80**, 174420 (2009).